JACS
JOURNAL OF THE AMERICAN CHEMICAL SOCIETY
Article
pubs.acs.org/JACS

Facile, Solution-Based Synthesis of Soft, Nanoscale Janus Particles with Tunable Janus Balance

André H. Gröschel,*[,†] Andreas Walther,[‡] Tina I. Löbling,[†] Joachim Schmelz,[†] Andreas Hanisch,[†] Holger Schmalz,[†] and Axel H. E. Müller*[,†]

[†]Makromolekulare Chemie II, Universität Bayreuth, D-95440 Bayreuth, Germany
[‡]DWI at RWTH Aachen University, D-52056 Aachen, Germany

Supporting Information

ABSTRACT: We present a novel, versatile, and simple solution-based routine to produce soft, nanosized Janus particles with tunable structural and physical properties at high volume yield. This process is based on the cross-linking of compartments within precisely defined multicompartment micelles (MCMs), which are themselves formed by the self-assembly of ABC triblock terpolymers. Therein, the C blocks form the stabilizing corona emanating from B compartments, which in turn reside on an A core. Cross-linking of the B compartments allows to permanently fixate the phase-separated state and dissolution in a good solvent for all blocks breaks up the MCMs into single Janus particles. They now consist of a core of cross-linked B blocks and two phase-separated hemispheres of A and C. The process gives access to unprecedented structural features such as tunable core diameter and control over the Janus balance ranging from dominant A side to equal hemispheres to dominant C side. We demonstrate that this simple one-pot approach can be extended to a range of triblock terpolymers with different block lengths and block chemistries to furnish a library of tailor-made Janus particles with widely tunable physical properties. Such a diversity and simplicity has remained unreachable with our previously developed approach using the controlled cross-linking of bulk morphologies. We show that this new synthetic route can be upscaled to a high volume yield of 10 wt %, thereby enabling large-scale applications. We further demonstrate the effect of the Janus balance on colloidal self-assembly. Janus particles with a dominant hydrophobic and a small hydrophilic patch aggregate into large clusters in water, but merely di- or trimerize in chloroform.

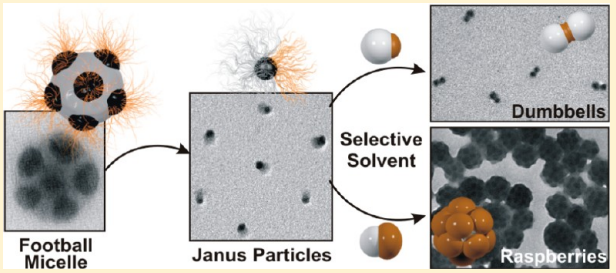

1. INTRODUCTION

Janus particles (JPs) are noncentrosymmetric spherical, cylindrical, or disk-like colloids feauring two phase-separated faces or compartments with distinct differences in chemical and/or physical properties.[1−3] Over the past two decades, JPs have drawn widespread attention in soft matter nanoscience[4] and materials science,[5,6] as nanomotors,[7−11] chemical or optical sensors,[12−20] for programmable self-assembly[21−24] and biomedical applications.[15−17,25] Especially their superior affinity toward interfaces, as compared to homogeneous particles, raised considerable interest for applications as future surfactants and for nanostructuring of interfaces.[3,26−28] Walther et al. showed that one single amphiphilic polystyrene-*block*-polybutadiene-*block*-poly(methacrylic acid) (SBMAA) Janus particle with a radius of 10 nm stabilizes ca. 100 × 100 nm^2 of an oil/water droplet interface and Binks et al. theoretically predicted a 2−3 times higher surface activity compared to surface isotropic particles.[29,30] The pronounced affinity toward interfaces makes JPs promising key building blocks for many technologically relevant applications, e.g., as surface coatings, stabilizers in emulsion polymerization or compatibilizers in polymer blends.[1,3,31−33] Depending on the nature of the particle, its hemispheres may selectively respond to solvent polarity, pH, electric field, or other stimuli to yield switchable materials. In combination with the surface anisotropy, these responsive properties allow for programmable, colloidal self-assembly, which is currently in focus of soft matter research.[21,23,34−37] The broken-symmetry renders JPs a unique particle class in the portfolio of patchy particles and complex colloids, in which shape and chemical anisotropy is used to impart molecule-like directionality for particle self-assemblies. For instance, very recently, Granick and co-workers reported on the directed self-assembly of amphiphilic, micrometer-sized JPs into nonequilibrium, complex triple helices by selective stimulation of the polyelectrolyte hemisphere with salt and kinetic selection of a self-assembly pathway.[38] This example unambiguously demonstrates the potential manifesting from the ability to control and understand the self-assembly behavior of JPs.

The influence of the Janus balance, i.e., the relative sizes of both hemispheres, has hardly been addressed so far, which is mainly due to difficulties in developing simple synthetic methods—particularly challenging on the nanoscale. Imple-

Received: June 18, 2012
Published: July 27, 2012

   dx.doi.org/10.1021/ja305903u | J. Am. Chem. Soc. 2012, 134, 13850−13860

Scheme 1. Self-Assembly of ABC Triblock Terpolymers into Multicompartment Micelles and Subsequent Disassembly into Janus Particles

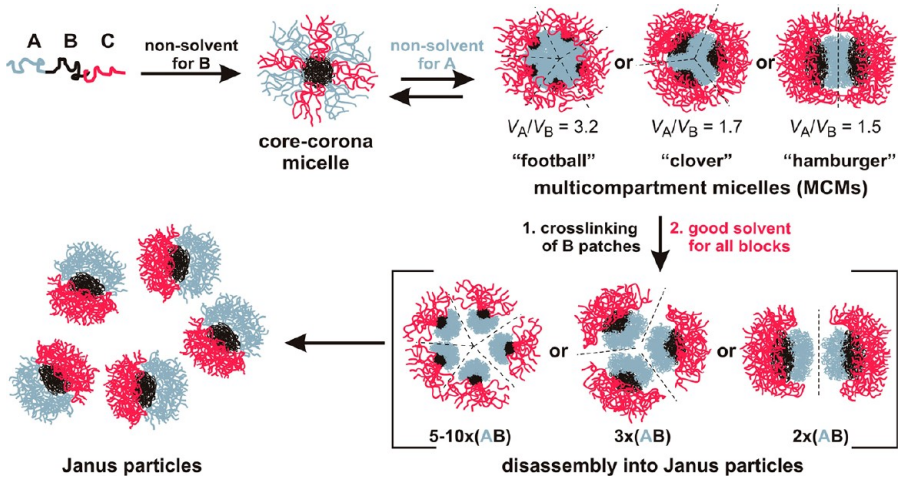

mentation of JPs with tunable Janus balance would, however, benefit the development and understanding of particle self-assembly into complex materials. Sophisticated self-assembly in selective solvents was already indicated in the early beginnings by Erhardt et al., who showed that SBMAA JPs self-assemble in water into clusters and supermicelles. In recent years, we further developed a comprehensive understanding of how different dimensionalities influence the self-assembly behavior by moving from spherical to cylindrical and disk-shaped JPs.[34,39−41]

Numerous synthetic strategies have been reported to produce purely inorganic,[42−45] polymer-inorganic hybrid JPs[35,45−48] as well as Janus polymersomes,[49] microgels,[47,50] droplets,[47,51,52] or fibers[53,54] in various shapes and geometries, mostly ranging from a few hundred nanometers to micrometers. However, only few reports were devoted to the synthesis of soft organic JPs on the nanoscale.[41,55−61] Up to now, the cross-linking of triblock terpolymer bulk morphologies has been the most capable and efficient method to fabricate polymer-based JPs of controllable size from 10 nm (Janus micelles) to several micrometers (Janus cylinders, tapes, discs, and sheets).[41,55,61,62] Although this method proved to be very successful over the past decade, the necessity of suitable polymer−polymer interaction parameters to enforce bulk segregation to the desired morphology limits the number of applicable polymers. This is especially pronounced for blocks in the weak segregation regime, e.g., for triblock terpolymers with short methacrylate blocks. Beyond that, casting, annealing, and cross-linking the bulk morphology can be a time-consuming process with some restrictions in scale-up. Solution-based approaches to nanosized JPs comprise template-assisted methods using desymmetrization tools, template-free formation of complex coacervate micelles of oppositely charged polymer blocks or unimolecular intramolecular polyelectrolyte complexation of a suitable triblock terpolymer.[58−60] However, in most cases tailored polymer block sequences, specific conditions or multistep processes considerably limit the number of materials that can be produced. It still remains a tremendous challenge to develop a versatile and simple method to produce soft, responsive, homogeneous JPs with nanoscale dimensions and tunable physical properties.[1]

In this report, we demonstrate how to overcome these problems and establish a novel solution-based strategy to prepare a range of chemically and structurally different JPs. We take advantage of our recently developed approach to uniform multicompartment micelles (MCMs)[63] formed by ABC triblock terpolymers in a stepwise, directed self-assembly process. The MCMs are constituted of cores of the A block, carrying compartments of the B block, and corona chains of the C block emanating from the B compartments (Scheme 1). The morphology can be directed to exclusively yield football, clover or hamburger MCMs (multiple, three or two B compartments) by adjusting the volume ratio, V_A/V_B, of the respective blocks. Cross-linking of the B compartments permanently fixates the phase-separated state and JPs are obtained after dissolution of the MCMs in a nonselective solvent. *No additional template or intermediate surface for desymmetrization is needed.* As a unique advantage of this procedure, we can prepare JPs with widely different volume fractions of blocks A and C and thus control the Janus balance. We show that the physical properties of the resulting JPs can be tuned by a number of polymer combinations suitable for this process. We follow the process using scattering and imaging techniques and analyze novel structural features such as tunable core radius and corona composition and its impact on the formation of colloidal superstructures. Finally, we demonstrate rapid synthesis on a larger scale and with high volume yields.

2. RESULTS AND DISCUSSION

2.1. Synthesis and Characterization of Janus Particles.

Homogeneity in both size and fine structure of the MCMs, as uniquely enabled by our directed self-assembly approach,[63] is decisive to synthesize uniform JPs via cross-linking of the B compartments and subsequent dissolution of the MCMs. We apply this new method to a wide range of triblok terpolymers as summarized in Chart 1. We first selected a range of polystyrene-*block*-polybutadiene-*block*-poly(methyl methacrylate) (SBM) triblock terpolymers to derive the effects of varying block weight fractions and overall molecular weight on the structure of the MCMs and the resulting JPs. Polystyrene-*block*-polybutadiene-*block*-poly(*tert*-butyl methacrylate) (SBT; P*t*BMA acts as a precursor for water-soluble polymethacrylic acid, PMAA) and polystyrene-*block*-polybutadiene-*block*-poly(2-vinylpyridine) (SBV) form JPs with amphiphilic corona hemispheres. Finally, poly(*tert*-butyl acrylate)-*block*-poly(2-cinnamoyloxyethyl acrylate)-*block*-poly(2-(dimethylamino)-

dx.doi.org/10.1021/ja305903u | J. Am. Chem. Soc. 2012, 134, 13850−13860

Chart 1. Chemical Structures of ABC Triblock Terpolymers[a]

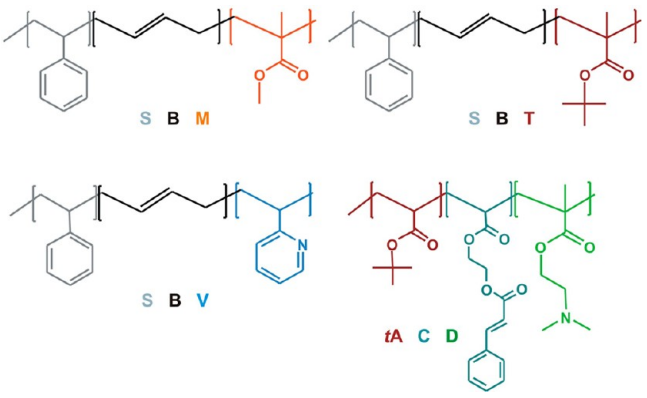

[a]S = polystyrene, B = polybutadiene, M = poly(methyl methacrylate), *t*A = poly(*tert*-butyl acrylate), T = poly(*tert*-butyl methacrylate), D = poly(2-(dimethylamino)ethyl methacrylate), C = poly(2-cinnamoyloxyethyl acrylate).

ethyl methacrylate) (*t*ACD) features completely different block chemistries. These particles give access to dipolar JPs with anionic and cationic hemispheres after deprotection of *t*A to poly(acrylic acid) and charge-up of D. It may be emphasized that the latter polymer is fully synthesized by controlled radical polymerization (here Atom Transfer Radical Polymerization), which can be easily accomplished with standard lab equipment. This represents some advantage compared to the stringent conditions needed for the anionic polymerization used to synthesize the other triblock terpolymers. The molecular characteristics of the triblock terpolymers such as block lengths, volume ratios, and the corona dimensions are summarized in Table 1 and Table S1 of the Supporting Information (SI).

The detailed mechanism of MCM formation is described in our previous report.[63] In the following, we shortly discuss the general mechanism to derive SBM JPs from SBM MCMs (Figure 1). The SBM triblock terpolymer is dispersed in a nonsolvent for the PB middle block to give core−corona micelles with a PB core and a patchy PS/PMMA corona. Subsequent dialysis of these core−corona micelles into a nonsolvent for both PS and PB initiates clustering into spherical MCMs. During this step, the corona patches (PMMA/PS) rearrange to minimize the energetically unfavorable PS/nonsolvent interface inducing aggregation along exposed PS patches. Depending on the block volume fractions, V_{PS}/V_{PB}, this yields MCMs with two, three, or multiple PB compartments, which we term "hamburger", "clover" or "football" MCMs, respectively. Within theses MCMs, the phase-separated state is permanently fixated by selective UV-cross-linking of the PB compartments with a photoinitiator. Subsequent redispersion in a good solvent for PS and PMMA breaks up the MCMs and liberates single, core-cross-linked SBM JPs. In a control experiment, we cross-linked the core−corona micelles (in the first selective solvent) prior to dialysis into the second solvent, which merely resulted in ill-defined aggregates. This can be attributed to the frozen, immobilized polymer chains after cross-linking and proves that only a mixed or patchy distribution of PS and PMMA chains is present in the first nonsolvent.[64,65] Thus, the self-assembly step into MCMs is essential to achieve complete phase separation and symmetry-breaking.

Figure 1 displays SBM2 "clover" MCMs with a discrete number of 3 PB compartments and very high regularity (over 92% trimers; Figure 1B). These were prepared via dispersion in *N*,*N*-dimethylacetamide (DMAc) to form micelles with a PB core and a patchyPS/PMMA corona and subsequent dialysis into acetone/isopropanol (70:30 v/v). After addition of a photoinitiator and selective UV-cross-linking of the PB compartments, we obtain single JPs in THF with a cross-linked PB core and hemispheres of PS and PMMA due to disassembly of the former MCMs.

According to ^{1}H NMR the signals for the double bonds completely disappear after cross-linking, while the PS to PMMA signal ratio remains constant (Figure S3 [SI]). These findings point to both a tight cross-linking and intact corona hemispheres (i.e., no radical cleavage or side reactions). The successful cross-linking was further confirmed by the detection of defined particles with a hydrodynamic radius of $\langle R_h \rangle_z = 36 \pm 4$ nm (PDI = 1.10) in THF via dynamic light scattering (DLS) (Table S1 and Figure S2 [SI]). The regular size distribution is corroborated by the corresponding TEM images depicting a very homogeneous population of JPs (Figure 1B). Most importantly, TEM imaging also gives an unambiguous proof of the Janus character, as the PS hemisphere clearly emanates as a gray shadow only from one side of the dark PB cores (OsO_4 staining: PS gray, PB black and PMMA not visible due to electron-beam degradation). Note that these gray patches are randomly oriented excluding drying artifacts (see also Figure 4B).

2.2. Control of the Core Size. Next, we use the series of SBM triblock terpolymers to deduce the relation between PB

Table 1. Characteristics of Triblock Terpolymers, Multicompartment Micelles and Janus Particles Used in This Study

code[a]	polymer[c]	MCM	*N*compartments	$R_{h,\,MCM}$ [nm][d]	$R_{h,\,JP}$ [nm][e]	R_{core} [nm][f]	f_{core} [wt %]	JB_A[g] [mol %]
SBM1	$S_{310}B_{150}M_{340}^{74}$	football	10−12	42 ± 6	19 ± 3	5.9 ± 1.2	11	47
SBM2	$S_{340}B_{330}M_{360}^{90}$	clover	3	36 ± 4	25 ± 4	10.9 ± 1.7	20	48
SBM3	$S_{610}B_{640}M_{290}^{127}$	large football	5−7	54 ± 5	35 ± 3	15.4 ± 2.3	27	68
SBM4	$S_{280}B_{330}M_{430}^{90}$	hamburger	2	37 ± 4	27 ± 3	10.4 ± 1.7	20	39
SBT[b]	$S_{510}B_{540}T_{350}^{132}$	clover	3	34 ± 3	30 ± 4	9.1 ± 1.6	22	59
SBV	$S_{360}B_{380}V_{590}^{120}$	clover	3	36 ± 4	29 ± 7	6.9 ± 1.3	17	38
*t*ACD	$tA_{190}C_{70}D_{110}^{59}$	hamburger/clover	2−3	36 ± 7	18 ± 3	8.1 ± 1.3	30	63

[a]For abbreviations see text and Chart 1. [b]Fraction of 1,4-butadiene units ~10 mol %; all SBM triblock terpolymers ~90 mol %. [c]Subscripts denote the number-average degree of polymerization and superscripts the overall molecular weight in kg/mol determined via combination of GPC using THF as the eluent and PS calibration and ^{1}H NMR spectroscopy. [d]MCMs measured at c = 1 g/L: SBM1−4 in acetone/isopropanol (70:30 v/v), SBT in ethanol, SBV in isopropanol and *t*ACD in pH 6 water. [e]*t*ACD JPs were measured in pH 3 water and all others in DMAc at c = 1 g/L (see Figure S1 in SI for distributions). [f]Average of 250 JP core radii determined by TEM image analysis. [g]JB_A describes the Janus balance as the molar fraction of block A in the corona: $JB_A = DP_{n,A}/(DP_{n,A} + DP_{n,C})$

dx.doi.org/10.1021/ja305903u | J. Am. Chem. Soc. 2012, 134, 13850−13860

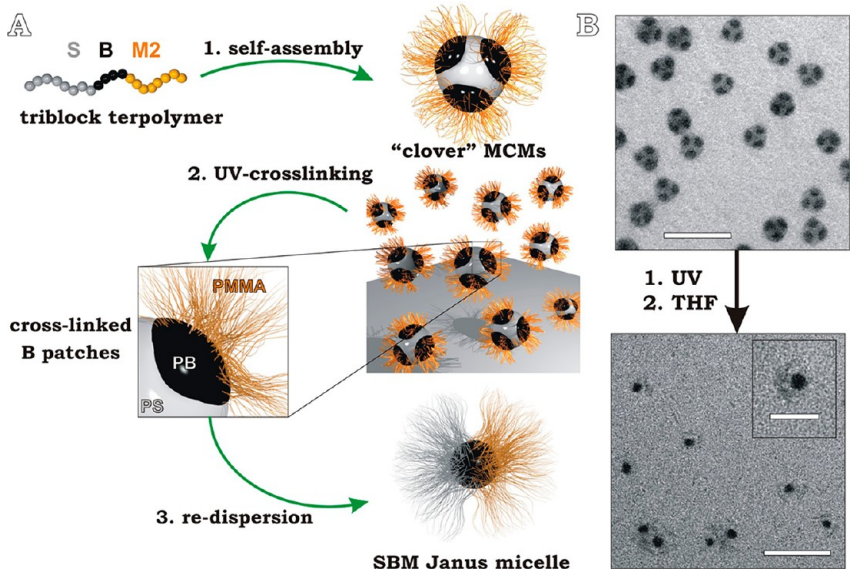

Figure 1. (A) JP synthesis via self-assembly of multicompartment micelles, subsequent cross-linking of the compartments and redispersion in THF. (B) Corresponding TEM images of SBM2 "clover" MCMs and derived JPs. OsO_4 staining: PS gray, PB black, and PMMA is not visible due to electron beam degradation. Scale bars are 200 and 50 nm in the inset.

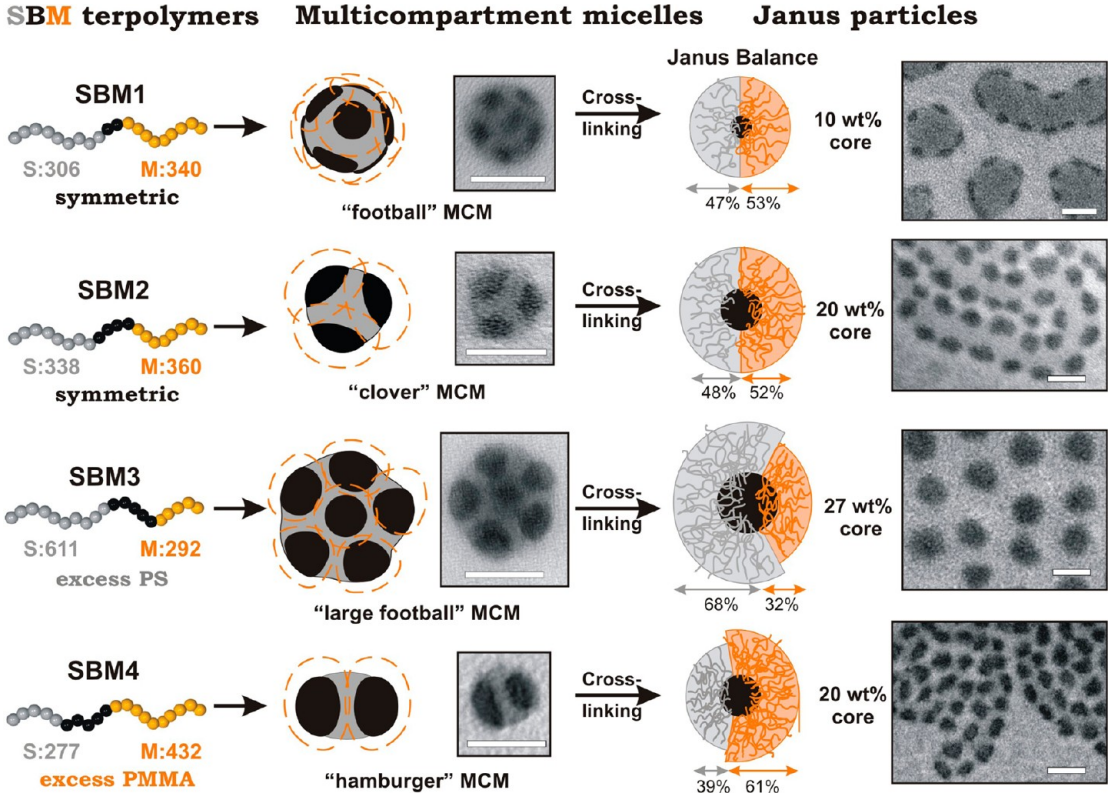

Figure 2. Tuning of core size and Janus balance of the JPs. TEM images of JPs obtained from THF solution. OsO_4 staining: PS gray, PB black, and PMMA is not visible due to electron beam degradation. Scale bars are 50 nm.

block length, $DP_{n,PB}$, and core radius, R_{core}, of the JPs (Figure 2). For this purpose, we synthesized JPs from SBM triblock terpolymers (SBM1, SBM2, and SBM3) with increasing block lengths of PB, $DP_{n,PB}$ = 150, 330, and 640. The TEM images of MCMs in the center column of Figure 2 already illustrate a size increase of the black PB compartments, which then effectively translates into larger core radii of the JPs after cross-linking.

An evaluation of 250 PB compartments for each sample yields sizes of R_{TEM} = 4.9 ± 1.0 nm for SBM1 "football" MCMs ($f_{PB} \approx 11$ wt %), R_{TEM} = 9.9 ± 1.7 nm for SBM2 "clover" MCMs ($f_{PB} \approx 20$ wt %) and R_{TEM} = 13.7 ± 1.9 nm for SBM3 "large football" MCMs ($f_{PB} \approx 27$ wt %). Note that especially in bulk morphologies, which have been pursued as source for SBM JPs so far, the weight fraction of the middle block usually cannot exceed 8−10 wt %, as otherwise spheres evolve into

dx.doi.org/10.1021/ja305903u | J. Am. Chem. Soc. 2012, 134, 13850−13860

Table 2. Relation Between Molecular Characteristics of the SBM Triblock Terpolymers and the Dimension of the PB Compartments in MCMs and the JPs Cores

code[a]	polymer[b]	M_{PB}^{chain} [kg/mol]	$DP_{n,PB}$	$R_{PB,MCM}$[c] [nm]	R_{core}[c] [nm]	$N_{agg,app}$[d]
SBM1	$S_{310}B_{150}M_{340}$	8.1	150	4.9 ± 1.0	5.9 ± 1.2	47 ± 28
SBM2	$S_{340}B_{330}M_{360}$	18.0	330	9.9 ± 1.7	10.9 ± 1.5	174 ± 81
SBM3	$S_{610}B_{640}M_{290}$	34.3	640	13.7 ± 1.9	15.1 ± 1.9	257 ± 115

[a]For abbreviations see text and Chart 1. [b]Subscripts denote the number-average degree of polymerization. [c]Determined from TEM of Janus particles cast from THF solution. [d]According to eq 1 in the Supporting Information.

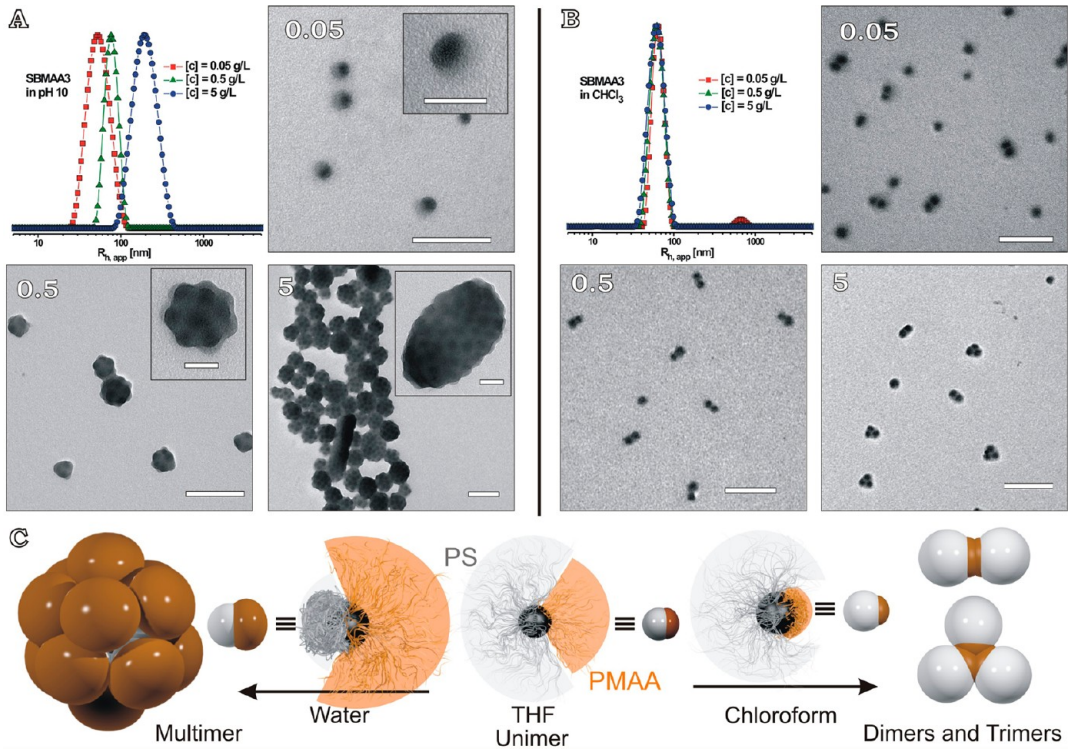

Figure 3. Self-assembly of SBMAA3 JPs in water and chloroform: (A) DLS size distributions and respective TEM images of clusters obtained after dialysis into water pH 10 at c = 0.05, 0.5, and 5 g/L. (B) DLS size distributions and respective TEM images of unimers to trimers in chloroform at c = 0.05, 0.5, and 5 g/L (OsO_4 staining: PS gray, PB black, PMMA not visible. Scale bars are 100 and 50 nm in insets). (C) Schematic clustering of asymmetric JPs in dependence of the corona size in chloroform and water pH 10. Here also, PS is gray and PB is black.

cylinders or lamellae.[66] Hence, nanoscale, soft JPs with such large core fractions (here up to f_{PB} = 27 wt %) can only be obtained with the presented solution approach. This is expected to be an important aspect for instance in Pickering emulsions as the desorption energy from an interface scales with the squared radius of the applied particles ($E \sim R^2$) and better nanoscale Pickering emulsifiers could be obtained by simply increasing the solid core radius, while maintaining the overall dimensions (core plus corona).

After cross-linking and redispersion in THF, all JPs exhibit slightly oblate ellipsoidal cores with radii correlating to the initial MCM compartments, as expected. We further evaluated the core radii of SBM JPs on basis of TEM images prepared from THF dispersions. Upon drying on the TEM grid, the particles partly self-assemble into characteristic patterns (Figure S4 [SI]). The PB cores are then located as black dots or ellipsoids at the interface between the PMMA-rich (bright) and the PS-rich (gray) phase. SBM3 preferably orients with one side to the hydrophobic carbon coating of the copper grid due to the favorable interactions with excess PS. The formation of these patterns does, however, not obstruct the evaluation of the sizes of the PB cores as summarized in Table 2 (average values of 250 core radii; see Figure S5 [SI] for distributions).

The core radii of our JP's follow a power law dependence on the PB block length with an exponent of x = 0.73 ± 0.10, which is in accordance with theoretical expectations for micelles intermediate between the star-like and crew-cut regime. Details are given in the Supporting Information (Figures S6 and S7).

2.3. Control of the Janus Balance. A characteristic feature of JPs, decisive for interfacial activity and self-assembly, is the ratio of surface phase-separation/compartmentalization, termed Janus balance, JB.[67] Recent studies showed that the free energy upon particle adsorption to water/oil interfaces can be significantly altered via the Janus balance.[30] In fact, very little effort has so far been devoted to understanding the influence of the JB on the type of self-assembled superstructure. This is to some extent due to the difficulties of tailoring this ratio with synthetic means. In our approach, we have a convenient molecular handle, encoded by precise macromolecular engineering, to distinctly manipulate this balance by simply modifying the A and C block lengths accordingly. In our MCM-based JPs, both patches have an identical number of polymer chains by definition. The ratio of monomer units of

dx.doi.org/10.1021/ja305903u | J. Am. Chem. Soc. 2012, 134, 13850−13860

both polymer chains is, at first approximation, sufficient to describe the symmetry or asymmetry of the two corona hemispheres. The contribution of one patch to the JB is then expressed by eq 1:

$$JB_A = \frac{DP_{n,A}}{DP_{n,A} + DP_{n,C}} \quad (1)$$

For instance, SBM2 JPs have symmetrical patches and we can quantify the contribution of the PS block to the Janus balance as JB_{PS} = 48% (or vice versa JB_{PMMA} = 52%). Assuming equal swelling of both corona blocks, also equal volumes of both hemispheres can be expected. On the contrary, SBM3 ($DP_{n,PS}$ = 610, $DP_{n,PMMA}$ = 290) and SBM4 ($DP_{n,PS}$ = 280, $DP_{n,PMMA}$ = 430) are triblock terpolymers with asymmetric end blocks. SBM3 JPs have a JB_{PS} = 68% and thus a dominant patch of PS, whereas SBM4 JPs have a JB_{PS} = 39% with a dominant patch of PMMA. Figure 2 schematically depicts the distribution and ratios of both corona patches.

2.4. Self-Assembly of Asymmetric PS-PB-PMAA (SBMAA) Janus Particles. JPs with equally sized patches (symmetric hemispheres) are expected to form the same equilibrium superstructures if brought into selective solvents for either side, because the conditions for aggregation are, in principle, identical in both cases. It stands to reason that asymmetric JPs will behave differently and self-assemble into clusters whose shape and size are strongly dependent on the patch size ratio (Janus balance) and the selective solvent. In the previous chapter we determined the Janus balance of SBM3 JPs to be JB_{PS} = 68% corresponding to a dominant PS patch. To enhance the solvent selectivity of the patches, we hydrolyzed the hydrophobic PMMA side to yield very hydrophilic poly(methacrylic acid) (PMAA). Self-assembly of the now strongly amphiphilic SBMAA3 JPs was then triggered by dialysis from THF, which is a solvent for both PS and PMAA, into either chloroform (selective for PS) or water pH 10 (selective for PMAA) (Figure 3).

We observe concentration-dependent self-assembly of the SBMAA3 JPs via the solvophobic PS patches, when dialyzed from THF into alkaline solutions. The TEM image series in Figure 3A shows a progressive increase in cluster size as a function of the JP concentration. Below a critical aggregation concentration, cac ≈ 0.05 g/L,[34] single JPs are the dominant species in TEM. DLS corroborates this finding as the $\langle R_h \rangle_z$ = 50 nm is in good agreement with the R_h obtained for single SBM3 JPs in THF ($\langle R_h \rangle_z$ = 49 nm). The Janus character is clearly visible from the gray PS shadow emanating from only one side of the black PB core (OsO_4 staining).

Considering the number of polymer chains per JP ($N_{agg,app}$ ≈ 260 for SBMAA3, Table 2 and SI) a molecular weight of several millions g/mol (M_{SBMAA3} ≈ 32 Mg/mol) is easily achieved for the Janus particles, and thus, the molar concentration at 0.05 g/L is only c ≈ 1.6 nmol/L. This low concentration reduces the probability of two JPs to aggregate during dialysis before the PMAA corona is progressively swelling and extended enough to provide complete shielding of the hydrophobic core (now PB + PS) against further aggregation. We observed a related behavior also in earlier studies on SBMAA Janus discs with much larger PS surfaces compared to those of the JPs here, where a substantial part of the Janus disks had PS surfaces unfavorably exposed to water.[40] Complete coverage of the hydrophobic core by PMAA chains can, in fact, be visualized via selective staining of the PMAA corona chains with uranyl acetate ($UO_2(OAc)_2$, see Figure S8 [SI]). Consequently, the Janus balance is inverted during the solvent exchange. If the concentration during dialysis is above the cac and two or more JPs are in close proximity or even in contact, the solvophobic PS patches undergo enough "effective" collisions and aggregate to minimize the unfavored PS/water interaction. At higher concentrations of 0.5 g/L, a fraction of JPs self-assemble into clusters consisting of 10−20 JPs reminiscent of their prior "football" MCM norphology (Figure 2). DLS measurements confirm clustering with an increase of the hydrodynamic radius to $\langle R_h \rangle_z$ = 89 nm. At a concentration of 5 g/L much larger aggregates are found with slightly elliptical shape and a cluster size typically exceeding 50 JPs ($\langle R_h \rangle_z$ = 194 nm). Note, that z-averaged hydrodynamic radii obtained by DLS overestimate larger particles and thus do not adequately represent the number-averaged size increase deduced from TEM. The polydispersity of these aggregates also increases with concentration, but individual JPs can no longer be found at 5 g/L.

To rationalize this behavior in terms of equilibrium or nonequilibrium self-assembly, one has to consider the time scales of dialysis and self-assembly, as well as the length scales of the JPs and corona arms and their dynamic changes. During solvent exchange, there is an interplay between the kinetics of particles colliding sufficiently often to form clusters and reach near-equilibrium aggregates, and the process of increasing swelling of PMAA and collapse of PS due to the continuous infiltration of water, arresting the growth potentially prematurely. The frequency of particle collisions per time is essentially controlled by their molar concentration, which is partly very low, thus requiring long equilibration times. The process of collapse and extension of solvophobic and solvophilic arms acts on a similar time scale for all concentrations but is decisive to induce kinetic control. In fact, the length scales of the JPs herein are peculiar, because the corona chains are sufficiently long to reach around the particle core, thus leading to an in situ change (here inversion) in Janus balance. Such a phenomenon cannot be expected for solid JPs with short ligands or large colloids grafted with polymers, in which the dimensions of the corona can be neglected compared to those of the solid core. Therefore, we deal with a complex self-assembly process, in which dynamic changes of the Janus balance and concentration-dependent reaction kinetics interact. Growth into near-equilibrium self-assemblies for a given Janus balance may only occur in a narrow window of solvent conditions and requires sufficient time. Here, this window rapidly closes due to continuously increasing water content, and rapid changes in the Janus balance hamper dynamics, efficient collisions, and further growth. Hence, the measured aggregates represent intermediate structures trapped in a nonequilibrium state. This is underscored by the fact that dilution of the large aggregates found at, e.g., 5 g/L does not lead to breakup into smaller clusters or individual micelles.

In contrast, when we dialyze the JPs from THF into chloroform, we only observe unimers to trimers in DLS and TEM (Figure 3B), almost independent of the concentration. Unlike in water, the hydrodynamic radius does not change, because the Janus balance does not undergo drastic changes during dialysis and the collapsed PMAA patch is completely protected by the much larger, expanded PS corona (Figure 3C). In concentration-dependent DLS measurements the hydrodynamic radii remain constant at $\langle R_h \rangle_z$ = 60 nm. Unimers, dimers, and trimers are the dominant species in TEM, which

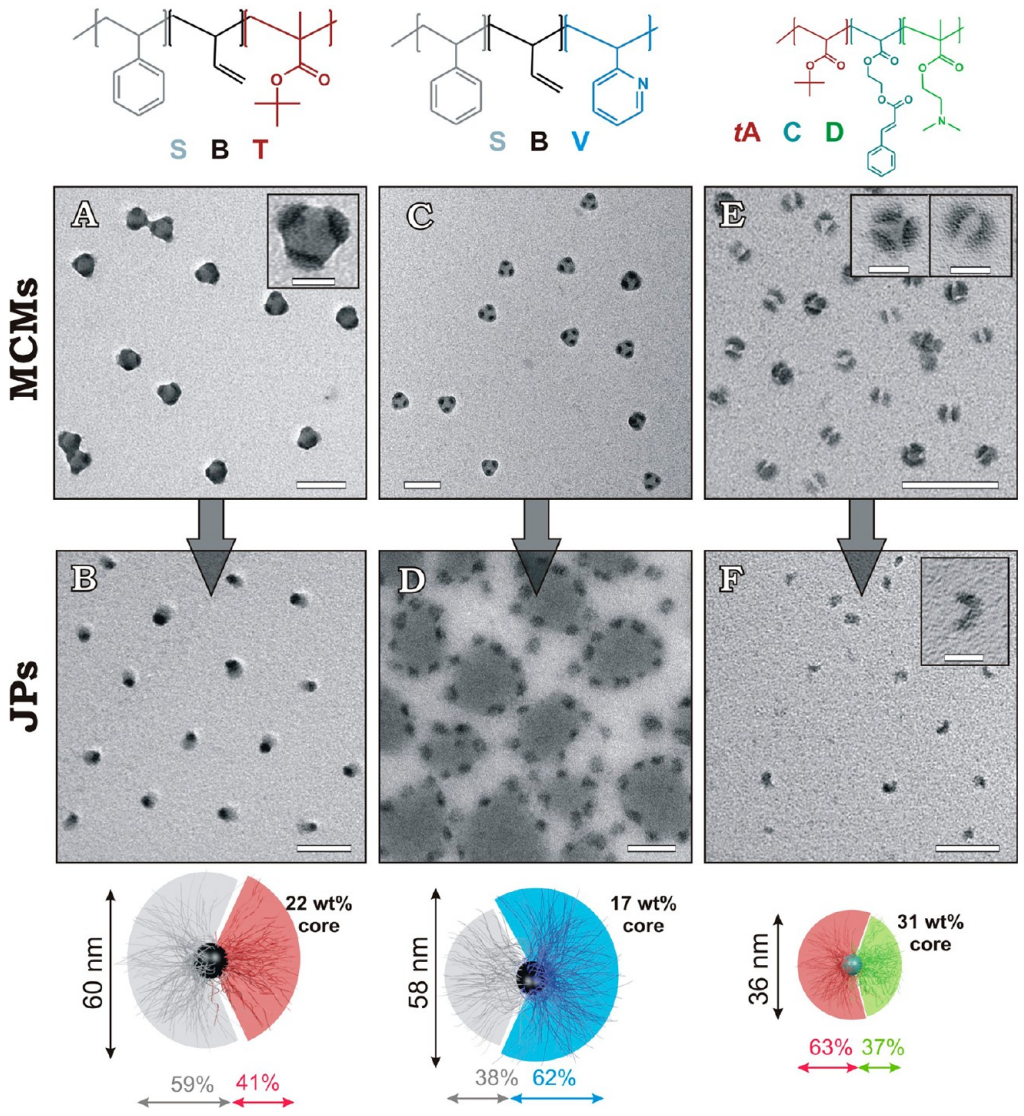

Figure 4. MCMs and resulting JPs after cross-linking: (A, B) SBT "clover" MCMs in ethanol and JPs in DMAc. (C, D) SBV "clover" MCMs in isopropanol and JPs in DMAc (A–D: OsO_4 staining: PS gray, PB black, P2VP dark gray and P*t*BMA not visible). (E, F) *t*ACD "clover" and "hamburger" MCMs at pH 6 and JPs at pH 3 (RuO_4 staining: PCEA black, P*t*BA bright gray and PDMAEMA not visible). All scale bars are 100 nm and 25 nm in the insets.

aggregate via the collapsed PMAA patch. The weaker solvophobic forces and the minor changes in Janus balance probably allow for an easier equilibration and the formation of near-equilibrium self-assemblies.

2.5. Generalization of the Concept. Another intriguing feature of the presented approach is the easy access to a multitude of chemistries in the corona hemispheres that so far remained inaccessible for a number of desired polymeric nanoscale JPs. Above, we already established the preparation of various SBM JPs. Next, we demonstrate the general applicability of our concept on the preparation of PS-PB-P*t*BMA (SBT), PS-PB-P2VP (SBV), and P*t*BA-PCEA-PDMAEMA (*t*ACD) JPs, following the same general protocol as described for SBM triblock terpolymers, except for the choice of solvents (Figure 4).

PS-PB-P*t*BMA (SBT) was first dispersed in DMAc as the nonsolvent for PB and annealed for 24 h at 70 °C. Except for the good solubility of P*t*BMA in alcohols, SBT triblock terpolymers are very similar in structure and polarity to those of SBM. Since PS is insoluble in alcohols, ethanol as a single solvent is sufficient to form stable "clover" MCMs with $\langle R_h \rangle_z$ = 34 ± 6 nm (Figure 4A). The SBT used here has almost identical block ratios (V_{PS}/V_{PB} = 1.7) as SBM2 and, as expected, the MCMs also contain three compartments with an abundance of >92%. After cross-linking, the JPs were redispersed in DMAc yielding $\langle R_h \rangle_z$ = 30 ± 9 nm (Figure S1, SI) with a core radius of R_{TEM} = 9.1 ± 1.6 nm in TEM (Figure 4B). According to the block lengths, we obtain JPs with a dominant PS patch (JB_{PS} = 59%) The Janus character is clearly visible as the gray PS patch exclusively emanates from one side of the black PB core (OsO_4 stained). The unfavorable interfacial tensions in the SBT system prevent a lamella–sphere bulk morphology even for very small fractions of PB[41] and, hence, SBT JPs are one example of an end block combination unique to this solution-based process.

The amphiphilic triblock terpolymer PS-PB-P2VP (SBV) was dispersed in DMAc as the nonsolvent for PB, annealed for 24 h at 70 °C, and then dialyzed into isopropanol (selective for P2VP). Self-assembly occurs via the insoluble PS patches into "clover" MCMs (Figure 4C). The cross-linked JPs were

dx.doi.org/10.1021/ja305903u | J. Am. Chem. Soc. 2012, 134, 13850–13860

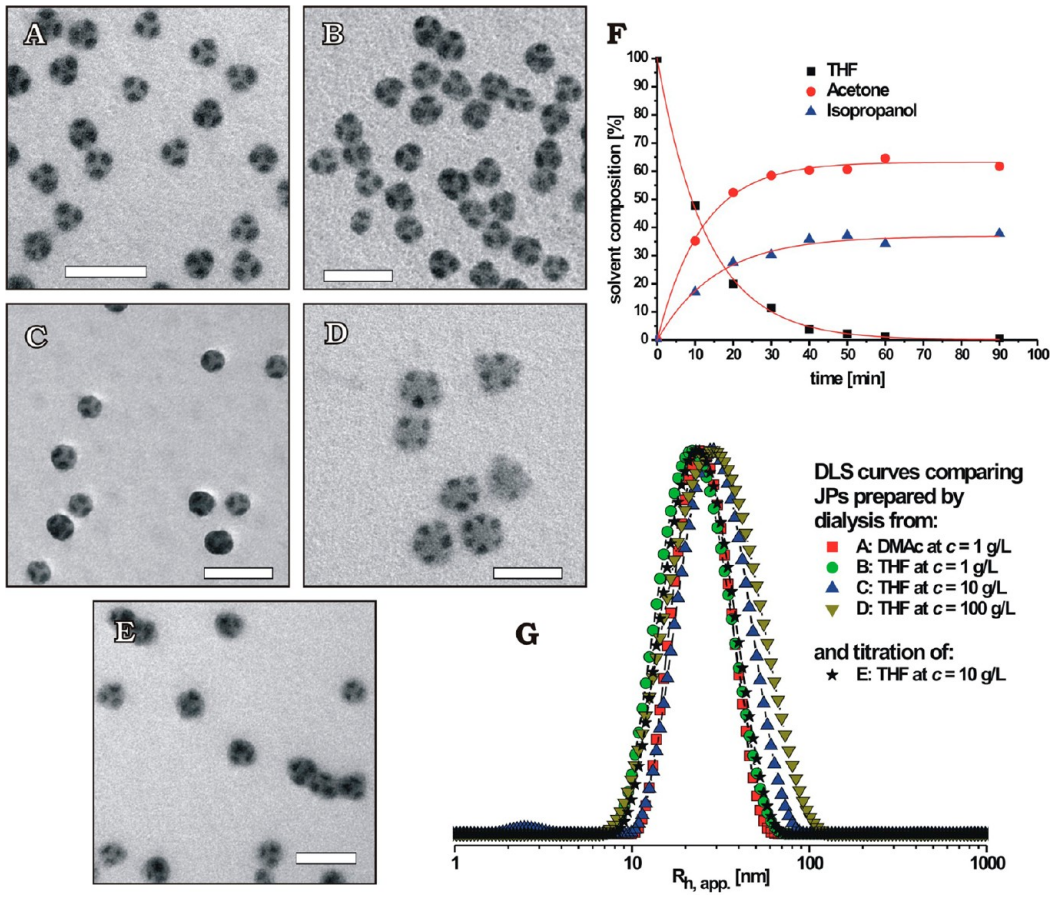

Figure 5. Influence of preparation protocol on MCM homogeneity: (A) SBM2 MCMs prepared via two-step dialysis at c = 1 g/L. (B–D) SBM2 MCMs prepared via direct dialysis of (B) 1 g/L, (C) 10 g/L, and (D) 100 g/L THF solutions against acetone/isopropanol (70:30 v/v). (E) SBM2 MCMs prepared via addition of acetone/isopropanol (70:30 v/v) to a 10 g/L SBM2 solution in THF (OsO_4 staining: PS gray, PB black, and PMMA not visible due to electron beam degradation. Scale bars are 100 nm). (F) ^{1}H NMR monitoring of the solvent composition during direct dialysis of 50 mL of a 1 g/L solution of SBM2 in THF into 5 L of acetone/isopropanol (70:30 v/v). (G) Intensity-weighted DLS size distributions of JPs prepared under different conditions (A–E) and measured in DMAc at c = 1 g/L after cross-linking.

redispersed in DMAc and measured with DLS ($\langle R_h \rangle_z$ = 29 ± 7 nm, Figure S1, SI) and TEM (R_{TEM} = 6.9 ± 1.3 nm, Figure 4D). Again both corona blocks (PS and P2VP) are soluble in DMAc, and JPs are identified in TEM, arranged in a circular fashion. It is evident that the black dots correspond to the PB core located at the interface of the dark gray P2VP and the bright gray PS phase. The JPs tend to aggregate along the P2VP patches upon drying on the TEM grid. The circular aggregation pattern may be attributed to the strong amphiphilic nature and the dominant P2VP patch with JB_{P2VP} = 62%. P2VP broadens the scope of JPs as it can be protonated or quaternized and easily gives access to hybrid materials by coordinating metals or semiconductor NPs. It may further serve in the buildup of inter-polyelectrolyte complexes with polyanions or anionic hemispheres of other JPs on the way to controlled colloidal self-assembly.

Finally, "clover" and "hamburger" MCMs of P*t*BA-PCEA-PDMAEMA (*t*ACD) with $\langle R_h \rangle_z$ = 36 ± 14 nm were prepared by direct dispersion in isopropanol (selective for *t*A and D) to form PCEA core micelles with a patchy P*t*BA/PDMAEMA corona and subsequent dialysis into water (pH = 6, selective for PDMAEMA). From earlier investigations we know that the PDMAEMA block poorly phase-separates in bulk from other poly(meth)acrylates. Yet, in solution this problem can be overcome as polymer–polymer interactions (bulk) are substituted by easily adjustable polymer–solvent interactions. RuO_4 selectively stains the aromatic groups of PCEA, and mostly 2–3 black PCEA compartments per MCM are clearly visible in TEM (Figure 4E). The cinnamoyl moieties of the PCEA block provide an attractive, additive-free cross-linking chemistry, as they are able to dimerize under UV-irradiation at a wavelength of λ_{max} = 300 nm.[69,70] After cross-linking, we imaged *t*ACD JPs in pH 3 (Figure 4F) with a core radius of R_{TEM} = 8.1 ± 1.3 nm (both PCEA and P*t*BMA are collapsed) and an $\langle R_h \rangle_z$ = 18 ± 3 nm in DLS. According to the block lengths, we obtain JPs with a dominant P*t*BA patch (JB_{PtBA} = 63%). The *t*ACD triblock terpolymer is a precursor for the fabrication of ampholytic, dipolar JPs responsive to changes in pH and temperature and at the same time exclusively composed of (meth)acrylate blocks synthesized via sequential ATRP.

2.6. Scale-Up. The demonstrated solution-based process is not only of academic significance, but also very attractive for fast and large-scale synthesis as needed in technological applications. SBM triblock terpolymers are, in fact, already commercially available, and their self-assembly is triggered solely by solvents that could be retrieved after precipitation of the JPs. Exemplified on SBM2, we demonstrate additional efforts to increase the volume yield and simplify production

dx.doi.org/10.1021/ja305903u | J. Am. Chem. Soc. 2012, 134, 13850–13860

(Figure 5). For reasons of simplicity we will focus on the MCM homogeneity as a measure of the final quality of the JPs.

Figure 5A shows SBM2 "clover" MCMs prepared via our dedicated two-step process furnishing most homogeneous MCMs. This typically involves dispersion in DMAc at a concentration of 1 g/L followed by dialysis into acetone/isopropanol (70:30 v/v). Controlled solvent transitions help to reduce kinetic barriers and facilitate the structural evolution from random coil to uniform MCMs. However, SBM2 MCMs can also be prepared faster in a single-step dialysis procedure, directly from THF into acetone/isopropanol (70:30 v/v), which leads to MCMs of good quality (Figure 5B). Further details on this "direct dialysis" approach can be found in our previous publication.[63] Benefits of this approach are utilization of THF as the starting solvent and the very fast replacement of THF with acetone/isopropanol, practically completed within one hour (Figure 5F). More importantly, the maximum output within a single production cycle can be considerably increased using very high concentrations. Although Figure 5D shows a higher number of compartments per MCM, the overall process is not disturbed as the blocks still show complete phase separation. This allows us to synthesize SBM2 JPs of reasonable quality by "direct dialysis" at significant concentrations of 10 wt % (100 g/L). Alternatively, dialysis can be avoided completely by direct addition of an excess of nonsolvent to a concentrated solution of the triblock terpolymer in THF. Such a titration method is commonly used to study micelle formation of block copolymers[71] and yields SBM2 MCMs of acceptable quality by adding 18 mL acetone/isopropanol (70:30 v/v) to 2 mL of a 10 g/L SBM2 solution in THF at a rate of 1 mL/min equaling a final concentration of 1 g/L (Figure 5E).

In Figure 5G we compare the DLS size distributions of JPs originating from MCMs that were prepared by the two-step dialysis, direct dialysis at concentrations of 1, 10, and 100 g/L and the described titration experiment to assess the quality of the JPs. The distributions of hydrodynamic radii reveal an excellent consistency and demonstrate that nearly identical JPs can be prepared while raising the concentration by 2 orders of magnitude and under accelerated and simplified preparation conditions. We observe a slight broadening of the distribution, potentially caused by the slightly less homogeneous PB compartments of the MCMs upon increasing concentration. Only direct dispersion of the triblock terpolymers in the final solvent or solvent mixture would be faster, but this method is typically not applicable to triblock terpolymers due to the long dissolution times for solvophobic blocks and the often resulting ill-defined structures.[63]

In summary, by applying these improvements, the entire production cycle can be reduced to only a few hours. Fast solvent exchange or even simple solvent addition combined with the possibility to use concentrated solutions of up to 100 g/L makes this procedure a meaningful candidate for production of tunable terpolymer-based JPs on a larger scale and further transfer into technologies.

CONCLUSION

We demonstrated a straightforward, solution-based approach to prepare Janus particles with widely tunable structural and physical properties by cross-linking uniform compartments of spherical multicompartment micelles (MCMs). The MCMs were derived from linear ABC triblock terpolymers in selective solvents by a stepwise self-assembly process. Templates or interfaces for desymmetrization are unnecessary. The core size of the Janus particles can be controlled by the length of the triblock terpolymer middle block. Further, we demonstrated that the concept applies to a range of triblock terpolymers and we expect validity to most polymer chemistries. Our method satisfies the need for the development of rapid and simple synthetic methods allowing functionality and responsiveness to be easily expanded, promoting the creation of comprehensive libraries.

Most importantly, the Janus balance (i.e., the relative volumes of the corona hemispheres) can be controlled by synthetically adjusting the lengths of the outer blocks of the terpolymers as they directly translate into the JP corona. We showed that the self-assembly of asymmetric Janus particles in selective solvents for the respective hemispheres leads to either a concentration-dependent cluster growth, when the majority of the corona is switched insoluble, or to an almost concentration-independent persistence of unimers, dimers and trimers when the minority of the corona is switched insoluble. The underlying complexity of this process is caused by competing dynamic changes of the Janus balance due to high volume ratios of corona to core, polymer dynamics that are influenced by the solvophobicity (from dynamic to frozen), and concentration-dependent reaction kinetics. The demonstrated self-assembly behavior and the question of non-equilibrium vs near-equilibrium self-assembly provides an intriguing glimpse into the emerging research field of self-assembly of patchy soft nanoobjects. Comprehensive studies on self-assembly of such asymmetric JPs with dynamic coronas are currently pursued by us and will be reported in due course.

This solvent-based, template-free approach will be a vital step toward further technological breakthroughs of Janus particles as it is simple, versatile and, in particular, scalable. This methodology brings about the necessary tools to tailor their core size and Janus balance and, in combination with macromolecular engineering, gives access to highly functional and responsive corona hemispheres. This can profoundly assist in a further understanding of the complex self-assembly of Janus particles and their use in applications.

ASSOCIATED CONTENT

Supporting Information

Methods and Materials, full Experimental Section, Polymer Characteristics, and further details on synthesis and characterization of the block copolymers using ^{1}H NMR, DLS, and TEM. This material is available free of charge via the Internet at http://pubs.acs.org.

AUTHOR INFORMATION

Corresponding Author

andre.groeschel@uni-bayreuth.de (A.H.G.); axel.mueller@uni-bayreuth.de (A.H.E.M.)

Notes

The authors declare no competing financial interest.

ACKNOWLEDGMENTS

This work was supported by the *Deutsche Forschungsgemeinschaft* within SFB 840 (TP A1 and A2) and Mu896/39-1. We thank Markus Müllner for helpful discussions.

REFERENCES

(1) Wurm, F.; Kilbinger, A. F. M. *Angew. Chem., Int. Ed.* **2009**, *48*, 8412−8421.

(2) Du, J.; O'Reilly, R. K. *Chem. Soc. Rev.* **2011**, *40*, 2402−2416.
(3) Walther, A.; Müller, A. H. E. *Soft Matter* **2008**, *4*, 663−668.
(4) de Gennes, P.-G. *Angew. Chem., Int. Ed.* **1992**, *31*, 842−845.
(5) Perro, A.; Reculusa, S.; Ravaine, S.; Bourgeat-Lami, E.; Duguet, E. *J. Mater. Chem.* **2005**, *15*, 3745−3760.
(6) Vanakaras, A. G. *Langmuir* **2005**, *22*, 88−93.
(7) Pavlick, R. A.; Sengupta, S.; McFadden, T.; Zhang, H.; Sen, A. *Angew. Chem., Int. Ed.* **2011**, *50*, 9374−9377.
(8) Wang, Y.; Hernandez, R. M.; Bartlett, D. J.; Bingham, J. M.; Kline, T. R.; Sen, A.; Mallouk, T. E. *Langmuir* **2006**, *22*, 10451−10456.
(9) Hong, Y.; Velegol, D.; Chaturvedi, N.; Sen, A. *Phys. Chem. Chem. Phys.* **2010**, *12*, 1423−1435.
(10) Ebbens, S. J.; Howse, J. R. *Langmuir* **2011**, *27*, 12293−12296.
(11) Baraban, L.; Makarov, D.; Streubel, R.; Mänch, I.; Grimm, D.; Sanchez, S.; Schmidt, O. G. *ACS Nano* **2012**, *6*, 3383−3389.
(12) Kretzschmar, I.; Song, J. H. *Curr. Opin. Colloid Interface Sci.* **2011**, *16*, 84−95.
(13) Nisisako, T.; Torii, T.; Takahashi, T.; Takizawa, Y. *Adv. Mater.* **2006**, *18*, 1152−1156.
(14) Kaufmann, T.; Gokmen, M. T.; Wendeln, C.; Schneiders, M.; Rinnen, S.; Arlinghaus, H. F.; Bon, S. A. F.; Du Prez, F. E.; Ravoo, B. J. *Adv. Mater.* **2011**, *23*, 79−83.
(15) Takei, H.; Shimizu, N. *Langmuir* **1997**, *13*, 1865−1868.
(16) Himmelhaus, M.; Takei, H. *Sens. Actuators, B* **2000**, *63*, 24−30.
(17) Behrend, C. J.; Anker, J. N.; McNaughton, B. H.; Brasuel, M.; Philbert, M. A.; Kopelman, R. *J. Phys. Chem. B* **2004**, *108*, 10408−10414.
(18) Erb, R. M.; Jenness, N. J.; Clark, R. L.; Yellen, B. B. *Adv. Mater.* **2009**, *21*, 4825−4829.
(19) Yin, S.-N.; Wang, C.-F.; Yu, Z.-Y.; Wang, J.; Liu, S.-S.; Chen, S. *Adv. Mater.* **2011**, *23*, 2915−2919.
(20) Behrend, C. J.; Anker, J. N.; Kopelman, R. *Appl. Phys. Lett.* **2004**, *84*, 154−156.
(21) Jiang, S.; Chen, Q.; Tripathy, M.; Luijten, E.; Schweizer, K. S.; Granick, S. *Adv. Mater.* **2010**, *22*, 1060−1071.
(22) Whitelam, S.; Bon, S. A. F. *J. Chem. Phys.* **2010**, *132*, 074901−074908.
(23) Smoukov, S. K.; Gangwal, S.; Marquez, M.; Velev, O. D. *Soft Matter* **2009**, *5*, 1285−1292.
(24) Hong, L.; Cacciuto, A.; Luijten, E.; Granick, S. *Nano Lett.* **2006**, *6*, 2510−2514.
(25) Millman, J. R.; Bhatt, K. H.; Prevo, B. G.; Velev, O. D. *Nat. Mater.* **2005**, *4*, 98−102.
(26) Walther, A.; Hoffmann, M.; Müller, A. H. E. *Angew. Chem., Int. Ed.* **2008**, *47*, 711−714.
(27) Ruhland, T. M.; Gröschel, A. H.; Walther, A.; Müller, A. H. E. *Langmuir* **2011**, *27*, 9807−9814.
(28) Glaser, N.; Adams, D. J.; Böker, A.; Krausch, G. *Langmuir* **2006**, *22*, 5227−5229.
(29) Binks, B. P.; Fletcher, P. D. I. *Langmuir* **2001**, *17*, 4708−4710.
(30) Aveyard, R. *Soft Matter* **2012**, *8*, 5233−5240.
(31) Pawar, A. B.; Kretzschmar, I. *Macromol. Rapid Commun.* **2010**, *31*, 150−168.
(32) Kim, S.-H.; Lee, S. Y.; Yang, S.-M. *Angew. Chem., Int. Ed.* **2010**, *49*, 2535−2538.
(33) Walther, A.; Matussek, K.; Müller, A. H. E. *ACS Nano* **2008**, *2*, 1167−1178.
(34) Erhardt, R.; Zhang, M.; Böker, A.; Zettl, H.; Abetz, C.; Frederik, P.; Krausch, G.; Abetz, V.; Müller, A. H. E. *J. Am. Chem. Soc.* **2003**, *125*, 3260−3267.
(35) Ling, X. Y.; Phang, I. Y.; Acikgoz, C.; Yilmaz, M. D.; Hempenius, M. A.; Vancso, G. J.; Huskens, J. *Angew. Chem., Int. Ed.* **2009**, *48*, 7677−7682.
(36) Cheng, L.; Zhang, G.; Zhu, L.; Chen, D.; Jiang, M. *Angew. Chem., Int. Ed.* **2008**, *47*, 10171−10174.
(37) Nie, L.; Liu, S.; Shen, W.; Chen, D.; Jiang, M. *Angew. Chem., Int. Ed.* **2007**, *46*, 6321−6324.
(38) Chen, Q.; Whitmer, J. K.; Jiang, S.; Bae, S. C.; Luijten, E.; Granick, S. *Science* **2011**, *331*, 199−202.
(39) Walther, A.; Drechsler, M.; Rosenfeldt, S.; Harnau, L.; Ballauff, M.; Abetz, V.; Müller, A. H. E. *J. Am. Chem. Soc.* **2009**, *131*, 4720−4728.
(40) Walther, A.; Drechsler, M.; Müller, A. H. E. *Soft Matter* **2009**, *5*, 385−390.
(41) Walther, A.; André, X.; Drechsler, M.; Abetz, V.; Müller, A. H. E. *J. Am. Chem. Soc.* **2007**, *129*, 6187−6198.
(42) Liang, F.; Shen, K.; Qu, X.; Zhang, C.; Wang, Q.; Li, J.; Liu, J.; Yang, Z. *Angew. Chem., Int. Ed.* **2011**, *50*, 2379−2382.
(43) Lin, C.-C.; Liao, C.-W.; Chao, Y.-C.; Kuo, C. *ACS Appl. Mater. Interfaces* **2010**, *2*, 3185−3191.
(44) Ye, S.; Carroll, R. L. *ACS Appl. Mater. Interfaces* **2010**, *2*, 616−620.
(45) Anderson, K. D.; Luo, M.; Jakubiak, R.; Naik, R. R.; Bunning, T. J.; Tsukruk, V. V. *Chem. Mater.* **2010**, *22*, 3259−3264.
(46) Liu, B.; Wei, W.; Qu, X.; Yang, Z. *Angew. Chem., Int. Ed.* **2008**, *47*, 3973−3975.
(47) Shepherd, R. F.; Conrad, J. C.; Rhodes, S. K.; Link, D. R.; Marquez, M.; Weitz, D. A.; Lewis, J. A. *Langmuir* **2006**, *22*, 8618−8622.
(48) Andala, D. M.; Shin, S. H. R.; Lee, H.-Y.; Bishop, K. J. M. *ACS Nano* **2012**, *6*, 1044−1050.
(49) Christian, D. A.; Tian, A.; Ellenbroek, W. G.; Levental, I.; Rajagopal, K.; Janmey, P. A.; Liu, A. J.; Baumgart, T.; Discher, D. E. *Nat. Mater.* **2009**, *8*, 843−849.
(50) Seiffert, S.; Romanowsky, M. B.; Weitz, D. A. *Langmuir* **2010**, *26*, 14842−14847.
(51) Nie, Z.; Li, W.; Seo, M.; Xu, S.; Kumacheva, E. *J. Am. Chem. Soc.* **2006**, *128*, 9408−9412.
(52) Lone, S.; Kim, S. H.; Nam, S. W.; Park, S.; Joo, J.; Cheong, I. W. *Chem. Commun.* **2011**, *47*, 2634−2636.
(53) Jung, J.-H.; Choi, C.-H.; Chung, S.; Chung, Y.-M.; Lee, C.-S. *Lab Chip* **2009**, *9*, 2596−2602.
(54) Srivastava, Y.; Marquez, M.; Thorsen, T. *Biomicrofluidics* **2009**, *3*, 012801.
(55) Erhardt, R.; Böker, A.; Zettl, H.; Kaya, H.; Pyckhout-Hintzen, W.; Krausch, G.; Abetz, V.; Müller, A. H. E. *Macromolecules* **2001**, *34*, 1069−1075.
(56) Butsele, K. V.; Fustin, C. A.; Gohy, J. F.; Jérome, R.; Jérome, C. *Langmuir* **2009**, *25*, 107−111.
(57) Li, Y.; Themistou, E.; Zou, J.; Das, B. P.; Tsianou, M.; Cheng, C. *ACS Macro Lett.* **2012**, *1*, 52−56.
(58) Zhang, S.; Li, Z.; Samarajeewa, S.; Sun, G.; Yang, C.; Wooley, K. L. *J. Am. Chem. Soc.* **2011**, *133*, 11046−11049.
(59) Voets, I. K.; de Keizer, A.; de Waard, P.; Frederik, P. M.; Bomans, P. H. H.; Schmalz, H.; Walther, A.; King, S. M.; Leermakers, F. A. M.; Cohen Stuart, M. A. *Angew. Chem., Int. Ed.* **2006**, *45*, 6673−6676.
(60) Cheng, L.; Hou, G.; Miao, J.; Chen, D.; Jiang, M.; Zhu, L. *Macromolecules* **2008**, *41*, 8159−8166.
(61) Liu; Abetz, V.; Müller, A. H. E. *Macromolecules* **2003**, *36*, 7894−7898.
(62) Wolf, A.; Walther, A.; Müller, A. H. E. *Macromolecules* **2011**, *44*, 9221−9229.
(63) Gröschel, A. H.; Schacher, F. H.; Schmalz, H.; Borisov, O. V.; Zhulina, E. B.; Walther, A.; Müller, A. H. E. *Nat. Commun.* **2012**, *3*, 710.
(64) Fang, B.; Walther, A.; Wolf, A.; Xu, Y.; Yuan, J.; Müller, A. H. E. *Angew. Chem., Int. Ed.* **2009**, *48*, 2877−2880.
(65) Schmelz, J.; Karg, M.; Hellweg, T.; Schmalz, H. *ACS Nano* **2011**, *5*, 9523−9534.
(66) Stadler, R.; Auschra, C.; Beckmann, J.; Krappe, U.; Voight-Martin, I.; Leibler, L. *Macromolecules* **1995**, *28*, 3080−3097.
(67) Jiang, S.; Granick, S. *J. Chem. Phys.* **2007**, *127*, 161102.
(68) Aveyard, R. *Soft Matter* **2012**, *8*, 5233−5240.
(69) Ding, J.; Liu, G. *Macromolecules* **1998**, *31*, 6554−6558.
(70) Lendlein, A.; Shastri, V. P. *Adv. Mater.* **2010**, *22*, 3344−3347.

(71) Walther, A.; Goldmann, A. S.; Yelamanchili, R. S.; Drechsler, M.; Schmalz, H.; Eisenberg, A.; Müller, A. H. E. *Macromolecules* **2008**, *41*, 3254−3260.